

Electronic Supporting Information

Oxidative dehalogenation of halophenols by high-valent nonheme iron(IV)-oxo intermediates

Umesh Kumar Bagha,^a Jagnyesh Kumar Satpathy,^a Gourab Mukherjee,^{a,b} Prasenjit Barman,^{a,c} Devesh Kumar,^{*d} Sam P. de Visser^{*a,e} and Chivukula V. Sastri^{*a}

^a Department of Chemistry, Indian Institute of Technology Guwahati, Assam 781039, India. Fax: +91-361-258-2349; E-mail: sastricv@iitg.ernet.in.

^b Department of Chemical Science, Tata Institute of Fundamental Research, Dr. Homi Bhabha Road, Colaba, Mumbai 400005, India.

^c Department of Chemistry, Kaliyaganj Collge, West Bengal, 733129, India

^d Department of Applied Physics, School for Physical Sciences, Babasaheb Bhimrao Ambedkar University, Lucknow 226025, India. E-mail: dkclcre@yahoo.com

^e The Manchester Institute of Biotechnology and Department of Chemical Engineering and Analytical Science, The University of Manchester, 131 Princess Street, Manchester M1 7DN, United Kingdom. E-mail: sam.devisser@manchester.ac.uk.

Table of Contents:

Part I: Experimental Data	Page S3
Part II: Characterization	Page S4
Part III: Kinetic Data	Page S5
Part IV: NMR Data	Page S8

Part I: Experimental Data.

Materials and methods

All Chemicals were obtained from Aldrich Chemical Co., and were of the best available purity and used without further purification unless otherwise stated. Solvents were dried according to published procedures¹ and distilled under argon prior to use. The substrate 2,4,6-trichlorophenol-D (2,4,6-TCP-D)², the ligand (2PyN2Q)³, the metal complex, [Fe^{II}(2PyN2Q)](CF₃SO₃)₂³⁻⁵ (**1**) and the iron(IV)-oxo intermediate⁶, [Fe^{IV}(O)(2PyN2Q)]²⁺(**2**) were synthesized using previously reported procedures. Then the intermediate **2** was further used for all the kinetic studies.

Instrumentation

The ¹H NMR spectra were recorded on a Bruker Avance III HD 500 MHz NMR spectrometers by using TMS as an internal standard. A Hewlett Packard 8453 spectrophotometer with a temperature controller either by a constant temperature water bath or a liquid nitrogen cryostat (Unisoku) was used to record UV-vis spectra. The ESI-MS spectra in the positive mode were recorded for the metal complex and the intermediate on an Agilent-Q-TOF 6520 instrument equipped with a Mass hunter workstation. Direct infusion of the samples into the source was done with the spray voltage at 3kV and a constant flow of drying gas at 5.0 L min⁻¹ at 200 °C. The X-band electron paramagnetic resonance (EPR) was measured on a JES-FA200 ESR spectrometer at 77 K in acetonitrile solution. EPR parameters: [frequency, 9136 MHz; power, 0.995 mW; field center, 490.00 mT, width, ±500.00 mT; sweep time, 30.0 s; modulation frequency, 100.00 kHz, width, 1 mT; amplitude, 1 mT, and time constant, 0.03 s].

Reactivity studies

All reactions were carried out in a 10 mm path length UV-vis cuvette by monitoring the change in UV-vis spectrum for the change in reaction solutions. The kinetics studies were performed in acetonitrile solvent at different temperatures depending upon the rate of reactivity of the intermediate with the halophenol substrates. The reactions were monitored by the change in characteristic absorption band as a function of time to obtain the pseudo first-order rate constants. The rate constants were evaluated by fitting the changes in absorbance of the intermediates under study. Reactions were run at least in triplicate and the data reported represent the average of those.

Product analysis

Products obtained in the dehalogenation reactions were analyzed by the ¹H NMR spectra using Bruker Avance III HD 500 MHz NMR spectrometers. After the completion of the reactions, the reaction mixtures were allowed to pass through a silica column and the products were collected in ethyl acetate. The collected solutions were subjected to dryness under a vacuum. The crude product was dissolved in CDCl₃ solvent and 1,2-dibromoethane was added as an internal standard to record the ¹H NMR spectra. The ratio of the percentage of dehalogenation products *ortho:para* quinones were quantified by comparing the NMR signals to those of authentic compounds.

Part II: Characterization

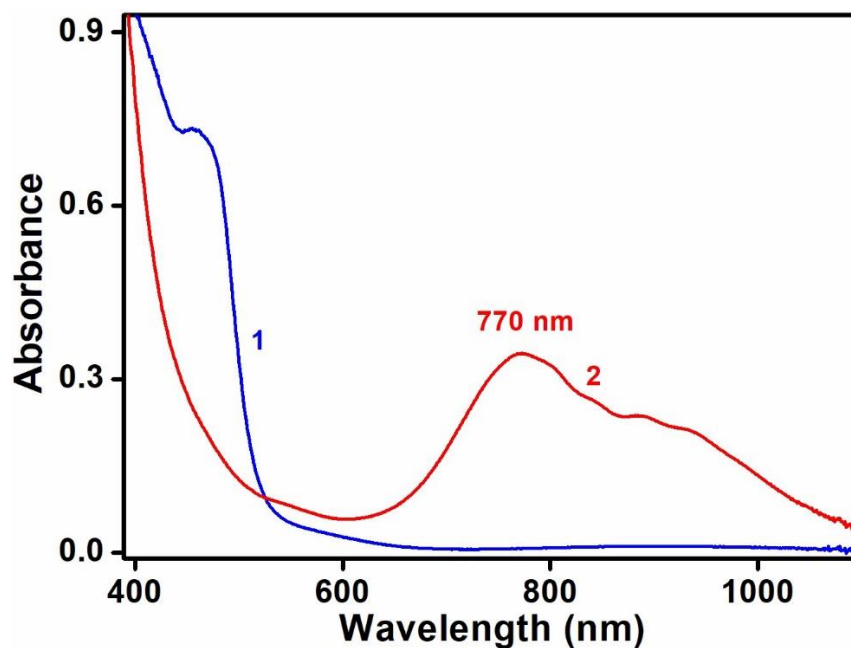


Fig.S1. UV-vis spectrum of $[\text{Fe}^{\text{II}}(2\text{PyN2Q})(\text{OTf})_2]$, **1** (blue line) and $[\text{Fe}^{\text{IV}}(\text{O})(2\text{PyN2Q})]^{2+}$, **2** (redline) in CH_3CN at 25 °C.

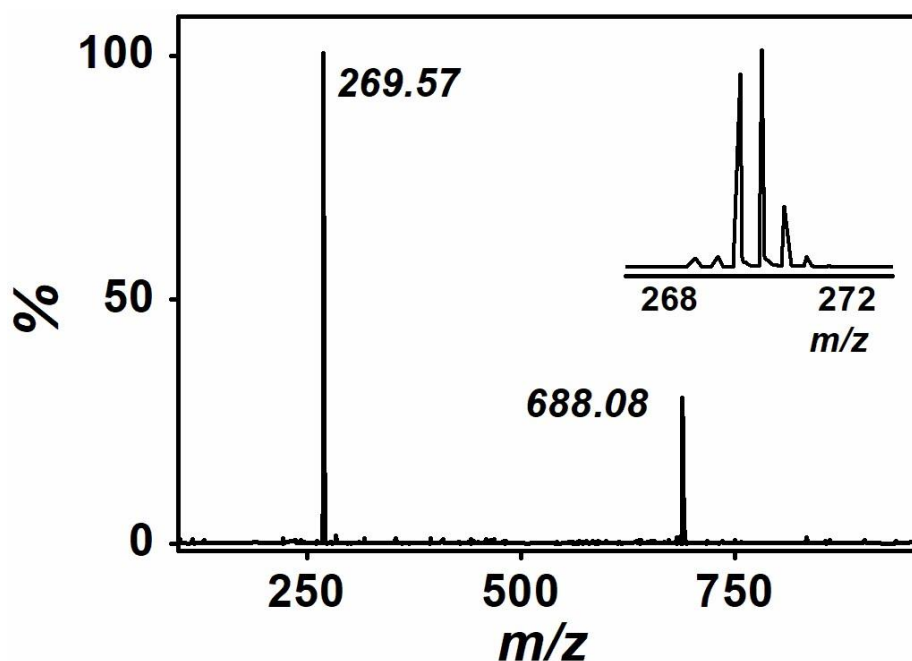


Fig. S2. Electrospray ionization mass spectra of **2**, in CH_3CN at 25 °C. The peaks at m/z 269.57 and 688.08 are assigned to $[\text{Fe}^{\text{IV}}(\text{O})(2\text{PyN2Q})]^{2+}$ and $[\text{Fe}^{\text{IV}}(\text{O})(2\text{PyN2Q})(\text{OTf})]^{1+}$ respectively. Inset shows the observed isotopic distribution pattern of m/z 269.57.

Part III: Kinetic Data

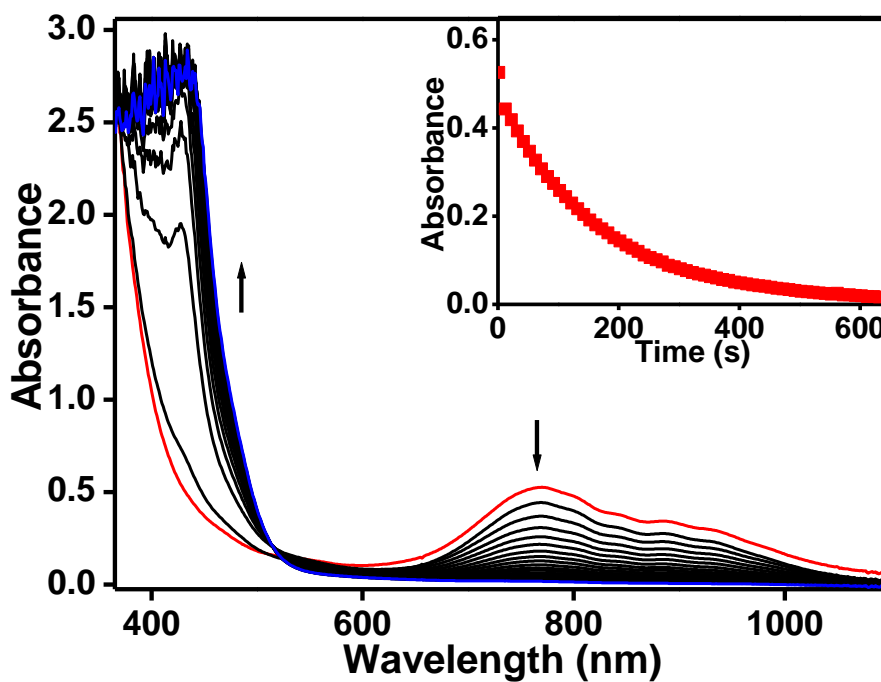


Fig. S3. UV-vis spectra of **2** upon addition of 10 equiv. of 2,6-DCP in CH₃CN at -40 °C. Inset shows the decay profile of the absorption band at 770 nm.

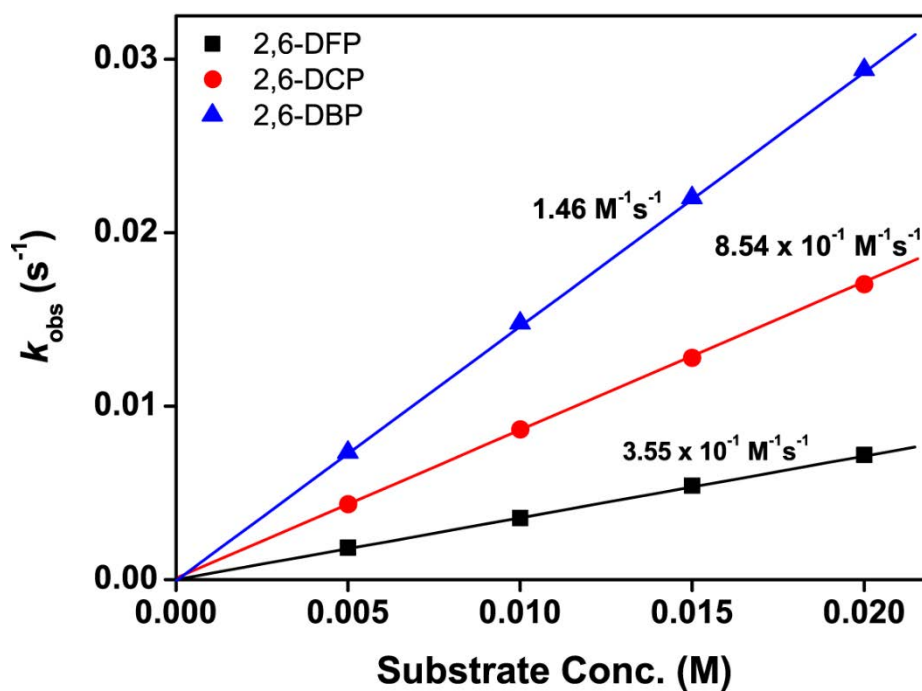


Fig. S4. second-order rate constants determined for **2** (1mM) with 2,6-DFP(■), 2,6-DCP(●) and 2,6-DBP (▲).

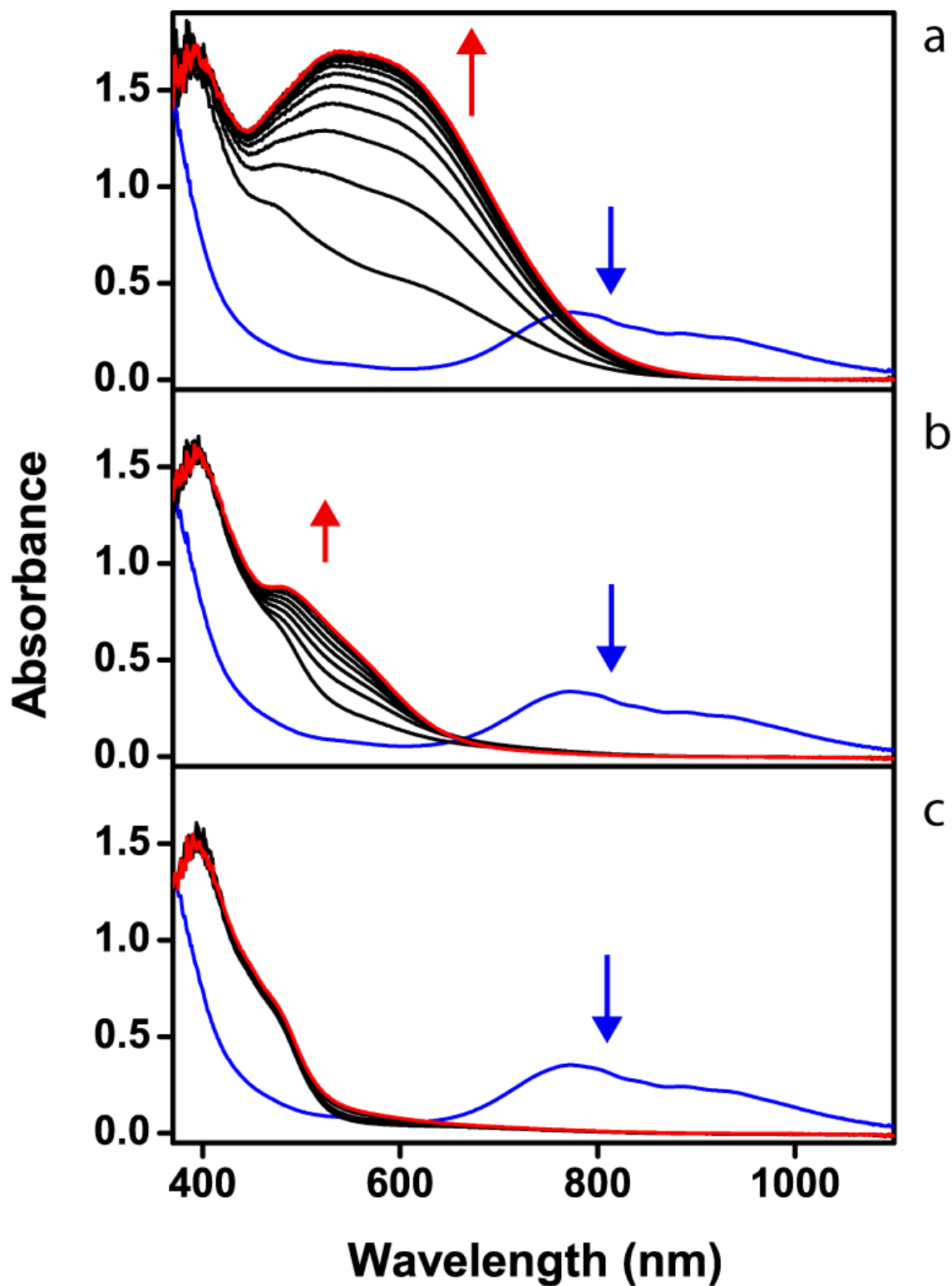


Fig. S5. UV-vis spectral changes of **2** upon addition of (a) 10 equiv. 2,4,6-TFP (b) 10 equiv. 2,4,6-TCP and (c) 10 equiv. 2,4,6-TBP in CH₃CN at room temperature. The formation of the adducts was observed for 400 s.

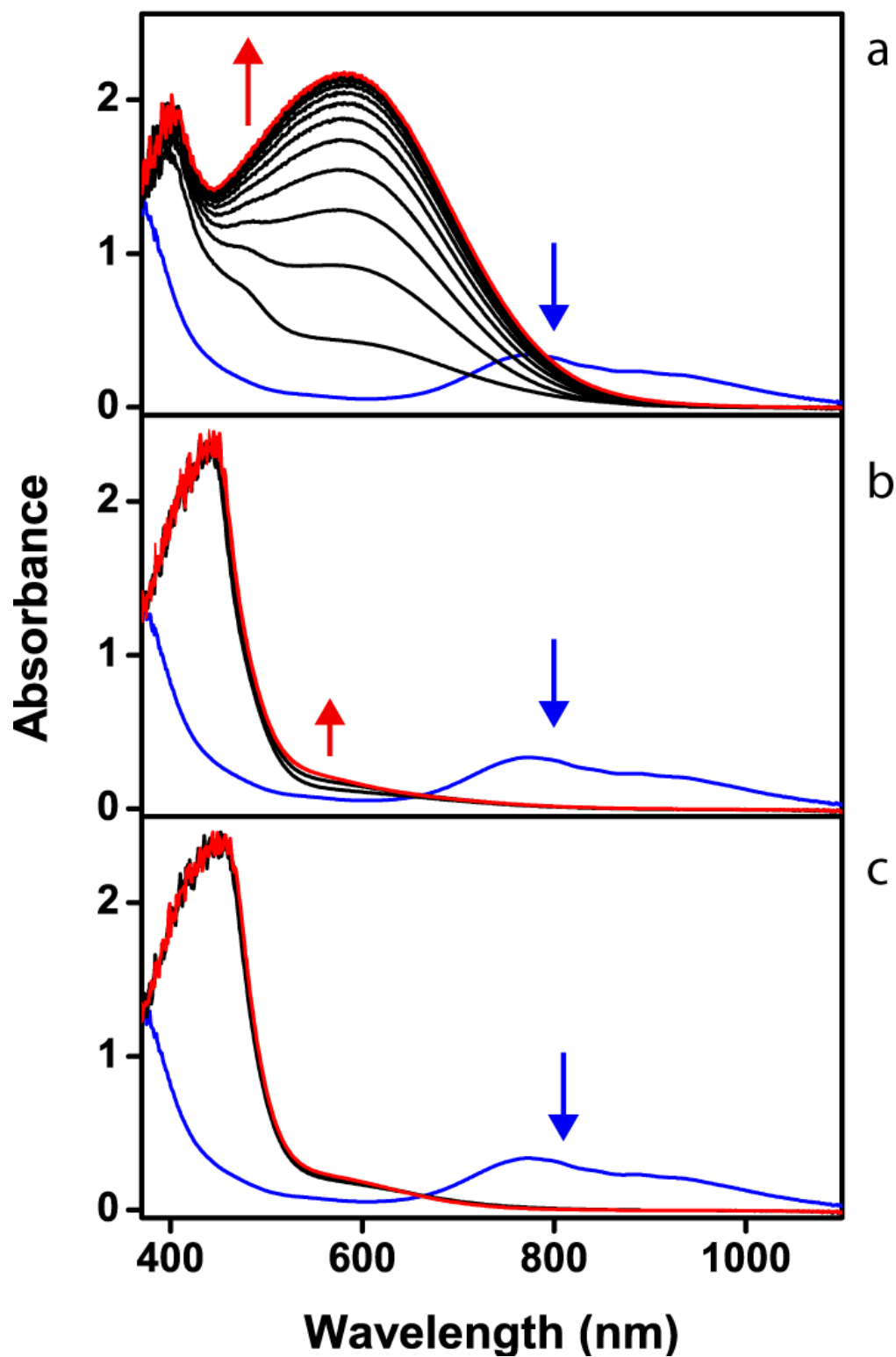


Fig. S6. UV-vis spectral changes of **2** upon addition of (a) 10 equiv. 2,6-DFP (b) 10 equiv. 2,6-DCP and (c) 10 equiv. 2,6-DBP in CH₃CN at room temperature. The formation of the adducts was observed for 400 s.

Part IV: NMR Data

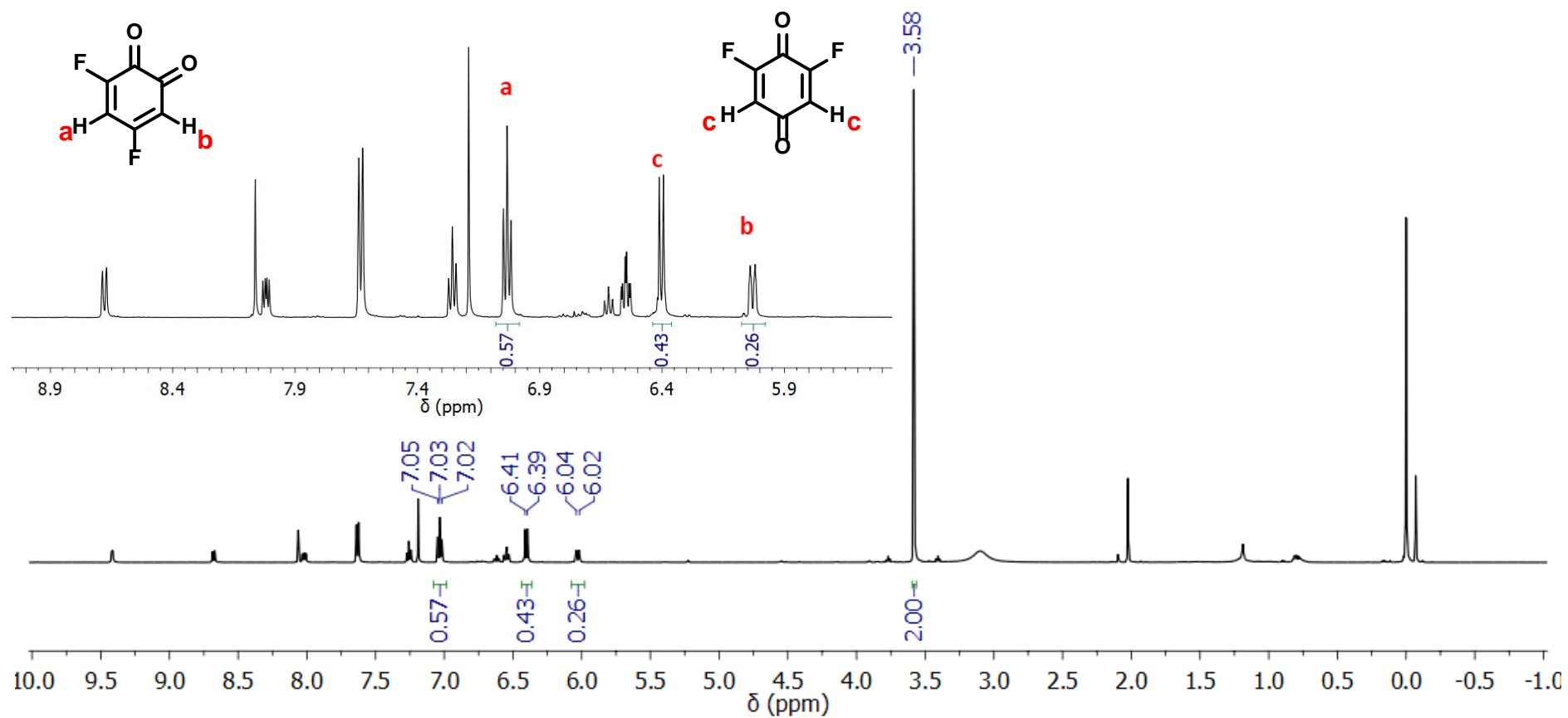


Fig. S7. ^1H NMR spectrum of reaction mixture of oxidized products of 2,4,6-trifluorophenol in CDCl_3 .

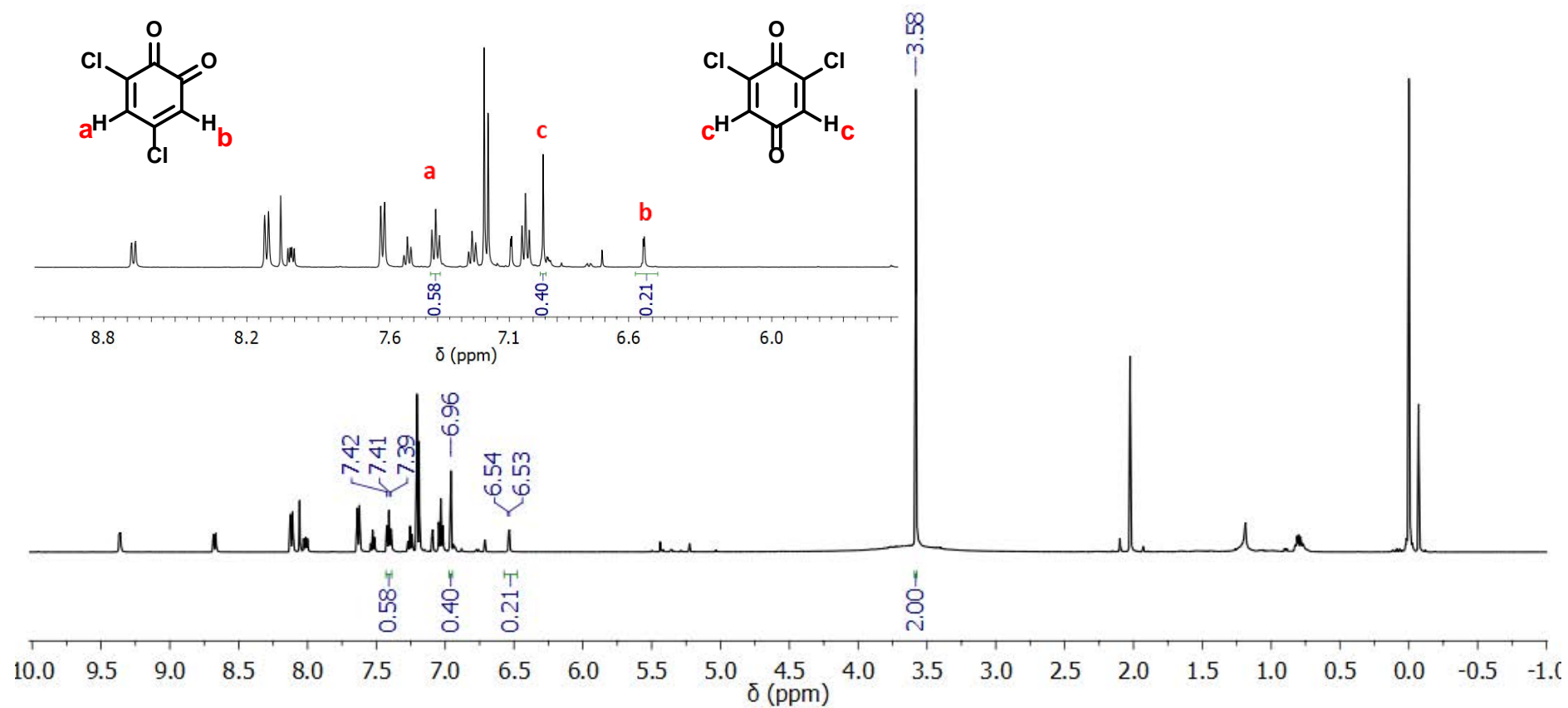


Fig. S8. ^1H NMR spectrum of reaction mixture of oxidized products of 2,4,6-trichlorophenol in CDCl_3 .

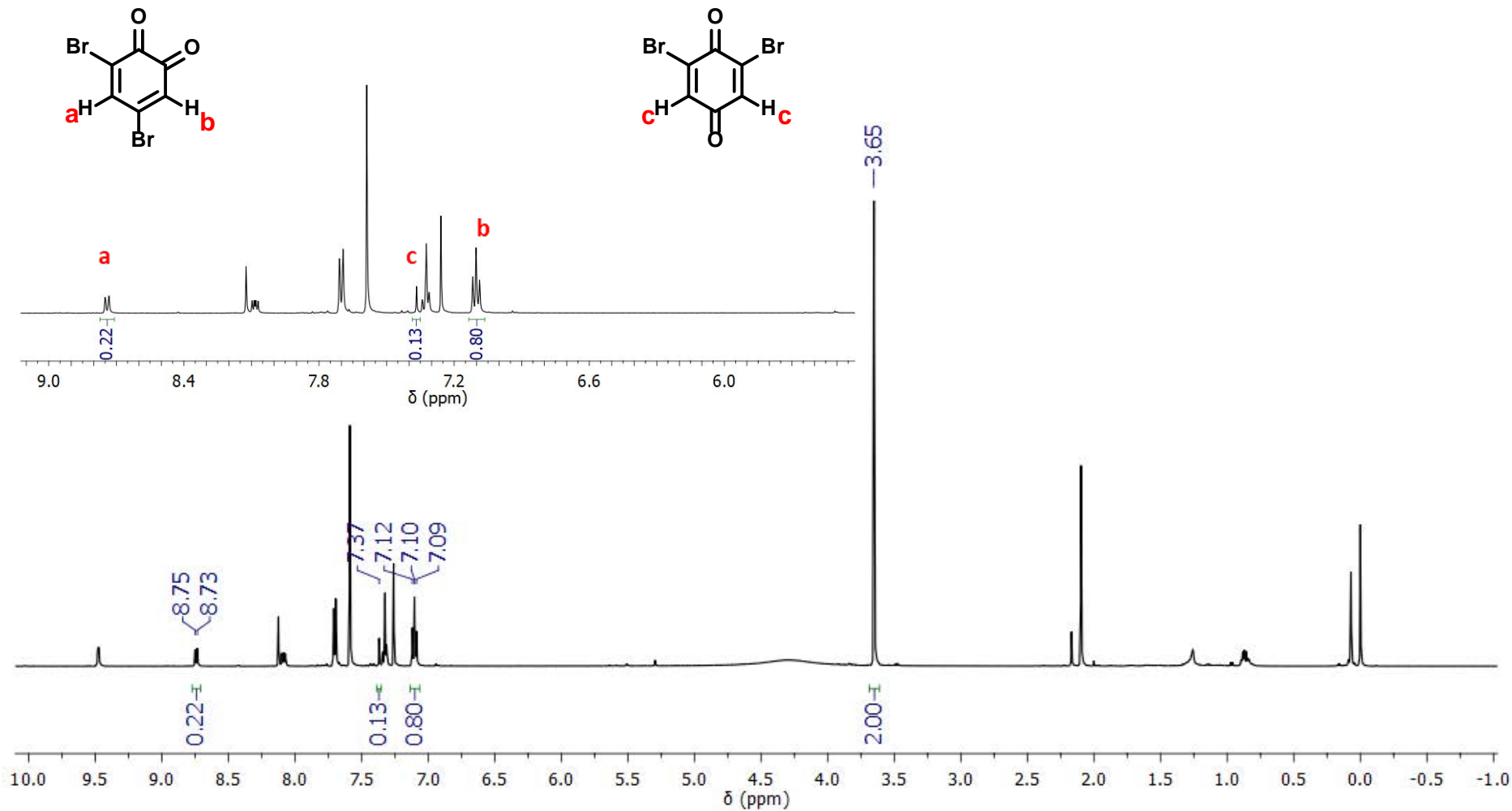


Fig. S9. ^1H NMR spectrum of reaction mixture of oxidized products of 2,4,6-tribromophenol in CDCl_3 .

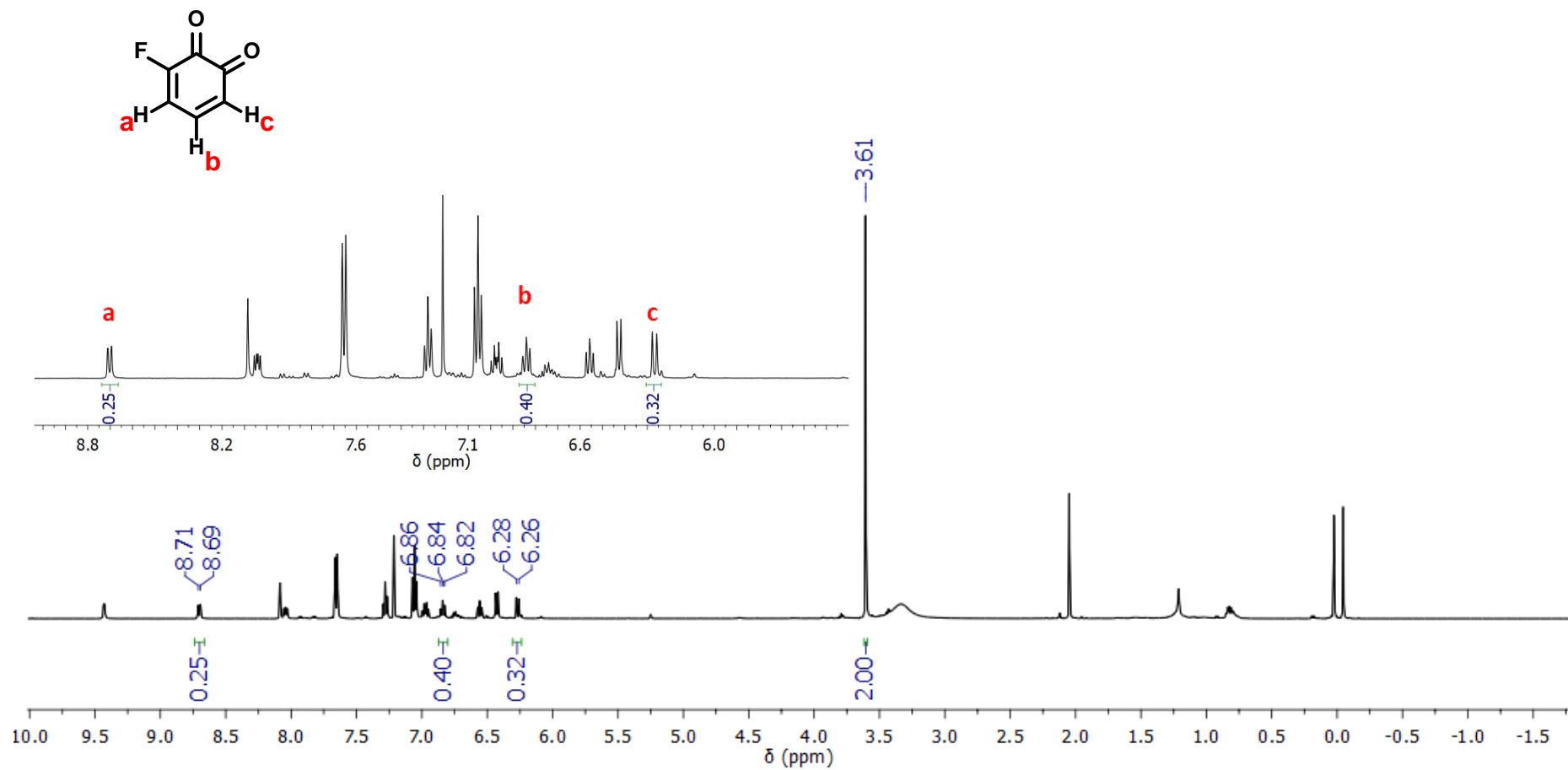


Fig. S10. ^1H NMR spectrum of reaction mixture of oxidized products of 2,6-difluorophenol in CDCl_3 .

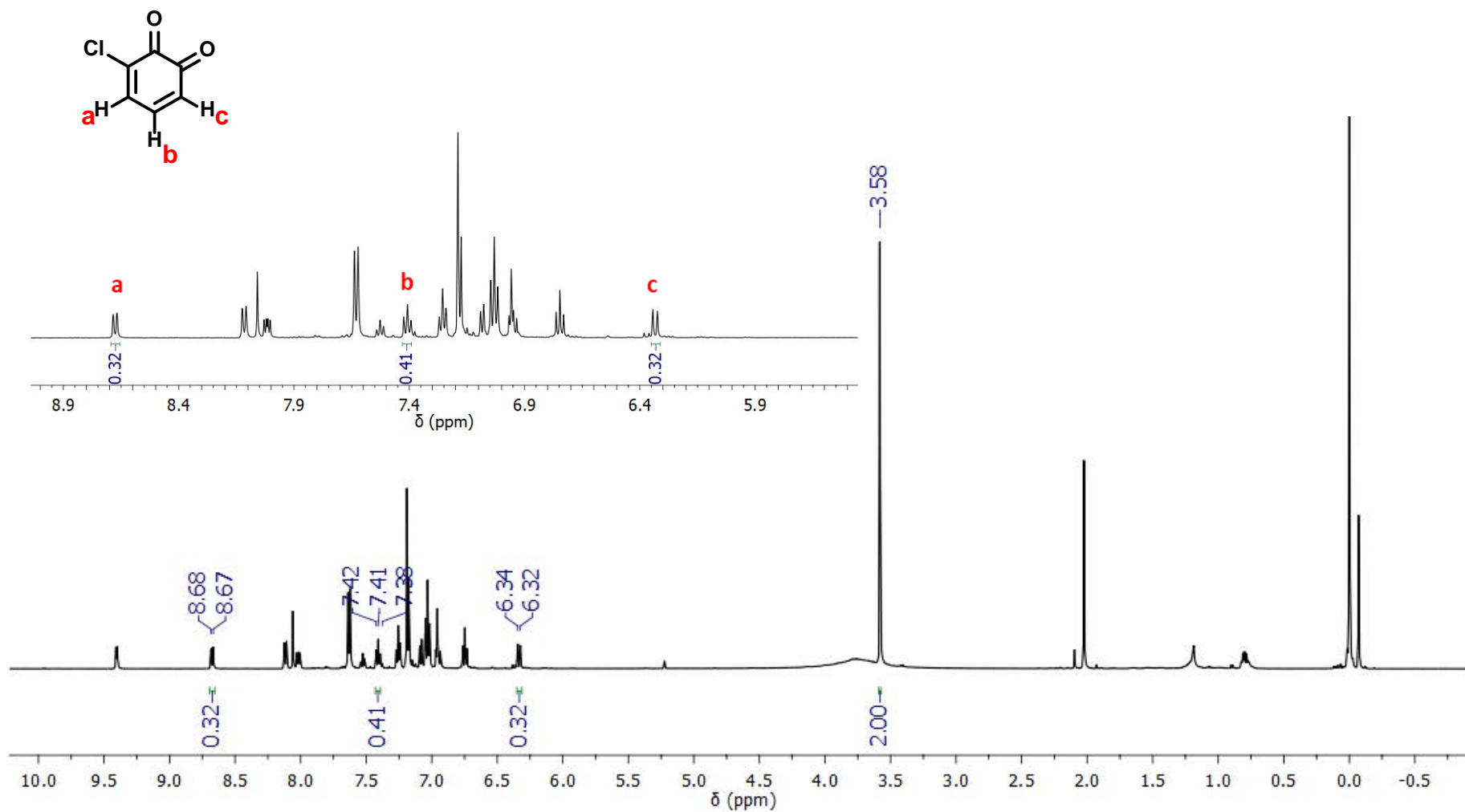


Fig. S11. ^1H NMR spectrum of reaction mixture of oxidized products of 2,6-dichlorophenol in CDCl_3 .

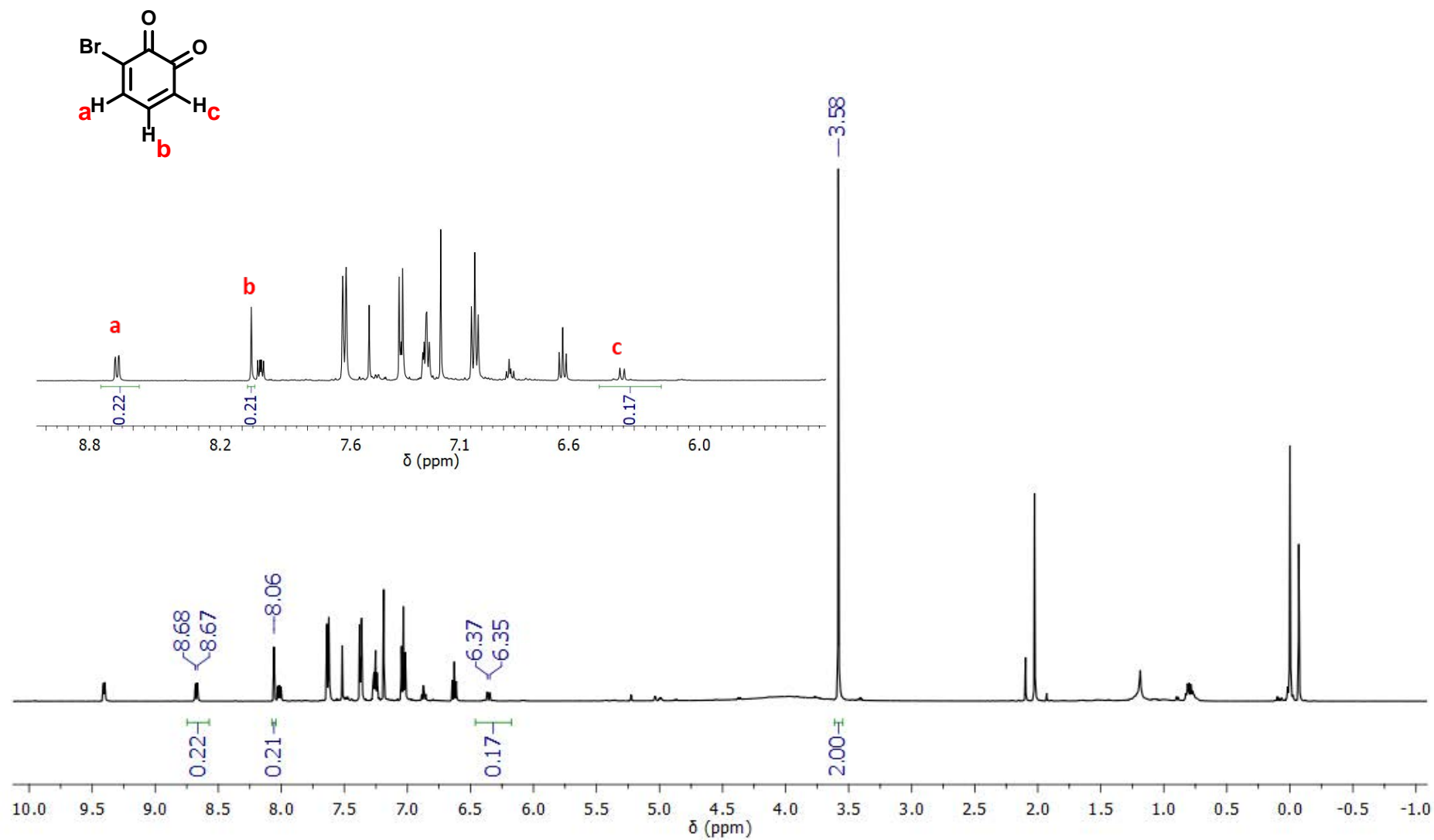


Fig. S12. ^1H NMR spectrum of reaction mixture of oxidized products of 2,6-dibromophenol in CDCl_3 .

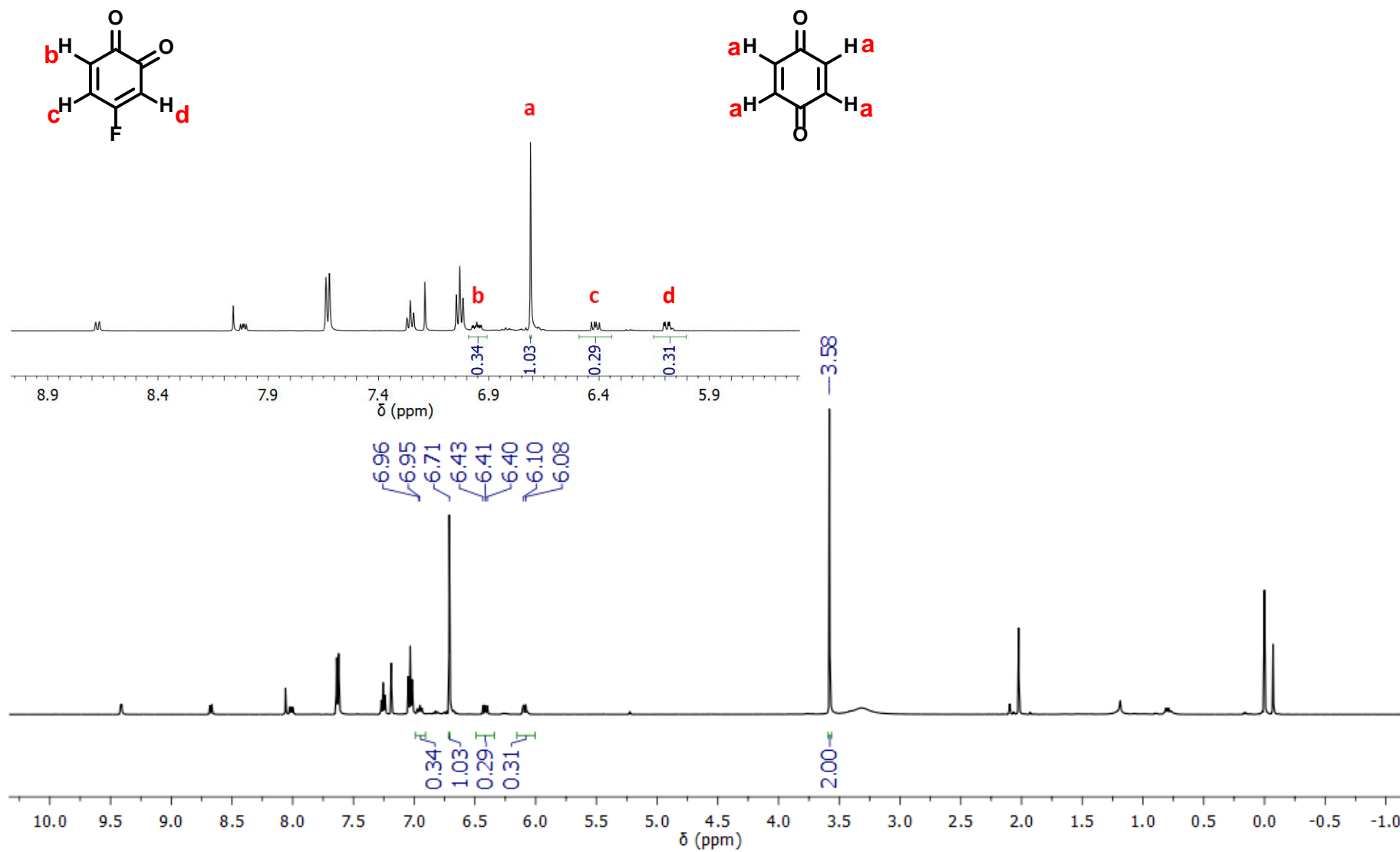


Fig. S13. ^1H NMR spectrum of reaction mixture of oxidized products of 4-fluorophenol in CDCl₃.

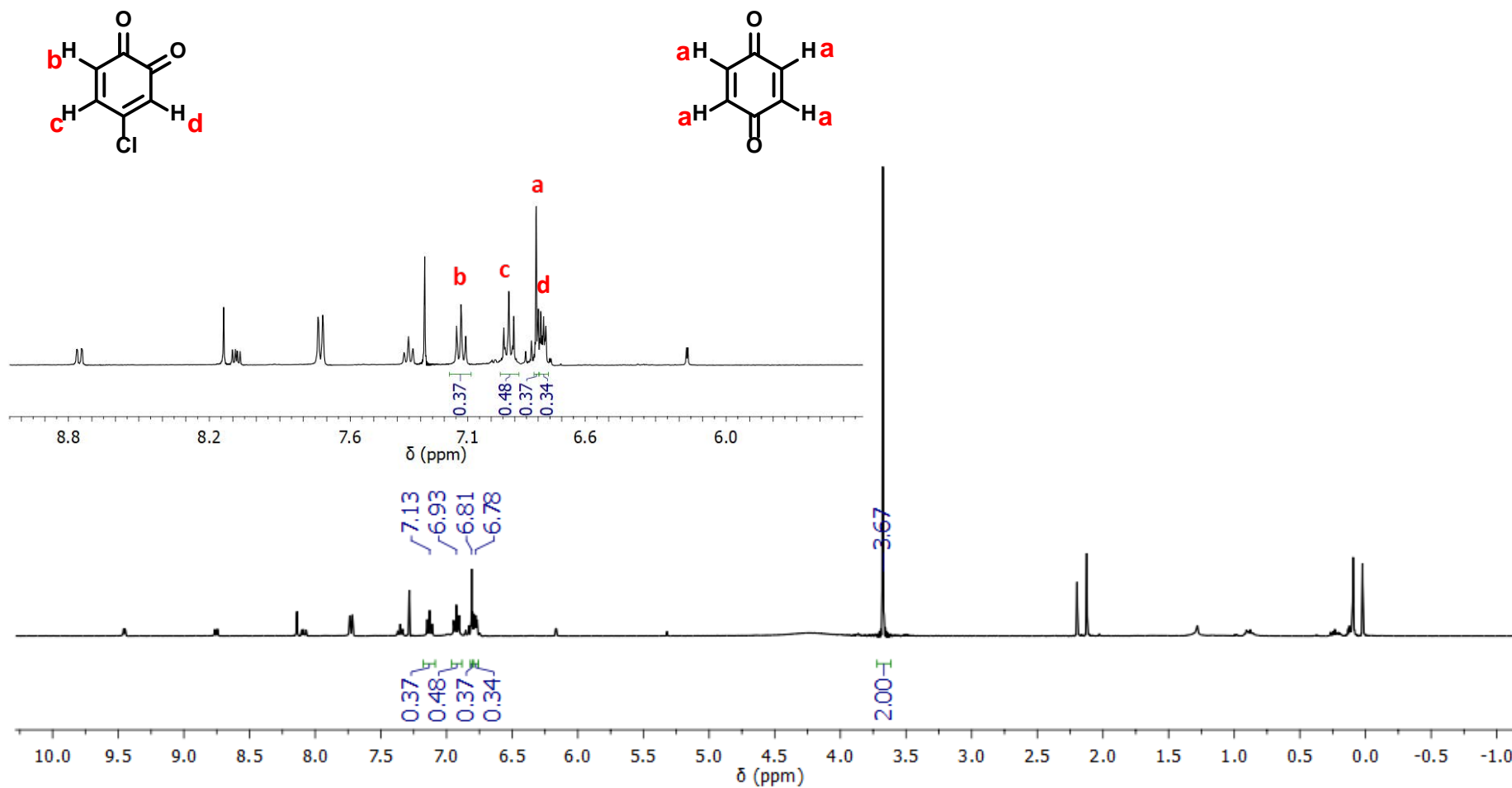


Fig. S14. ^1H NMR spectrum of reaction mixture of oxidized products of 4-chlorophenol in CDCl_3 .

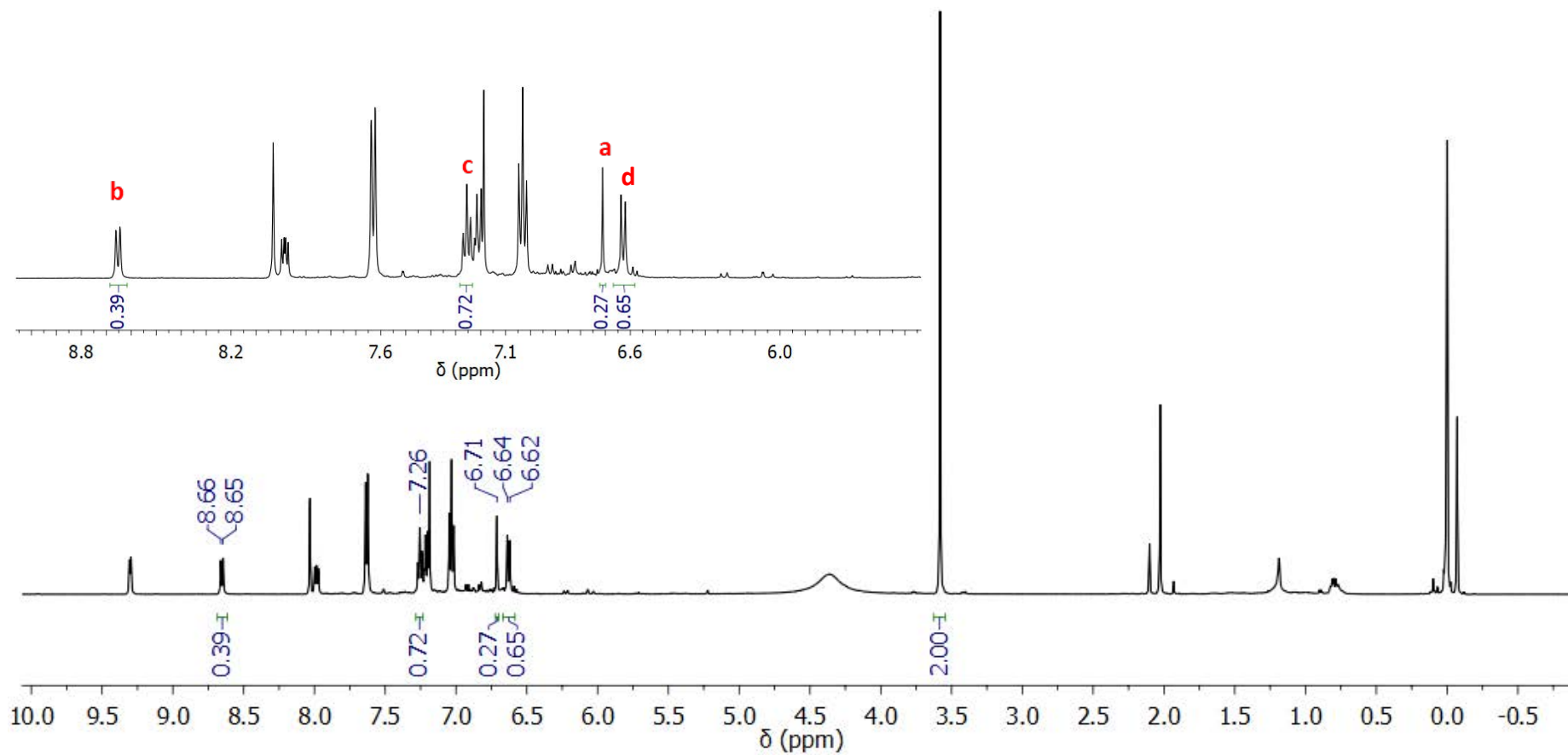
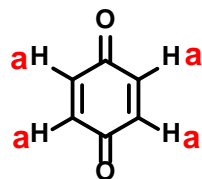
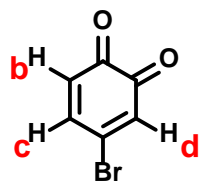


Fig. S15. ^1H NMR spectrum of reaction mixture of oxidized products of 4-bromophenol in CDCl_3 .

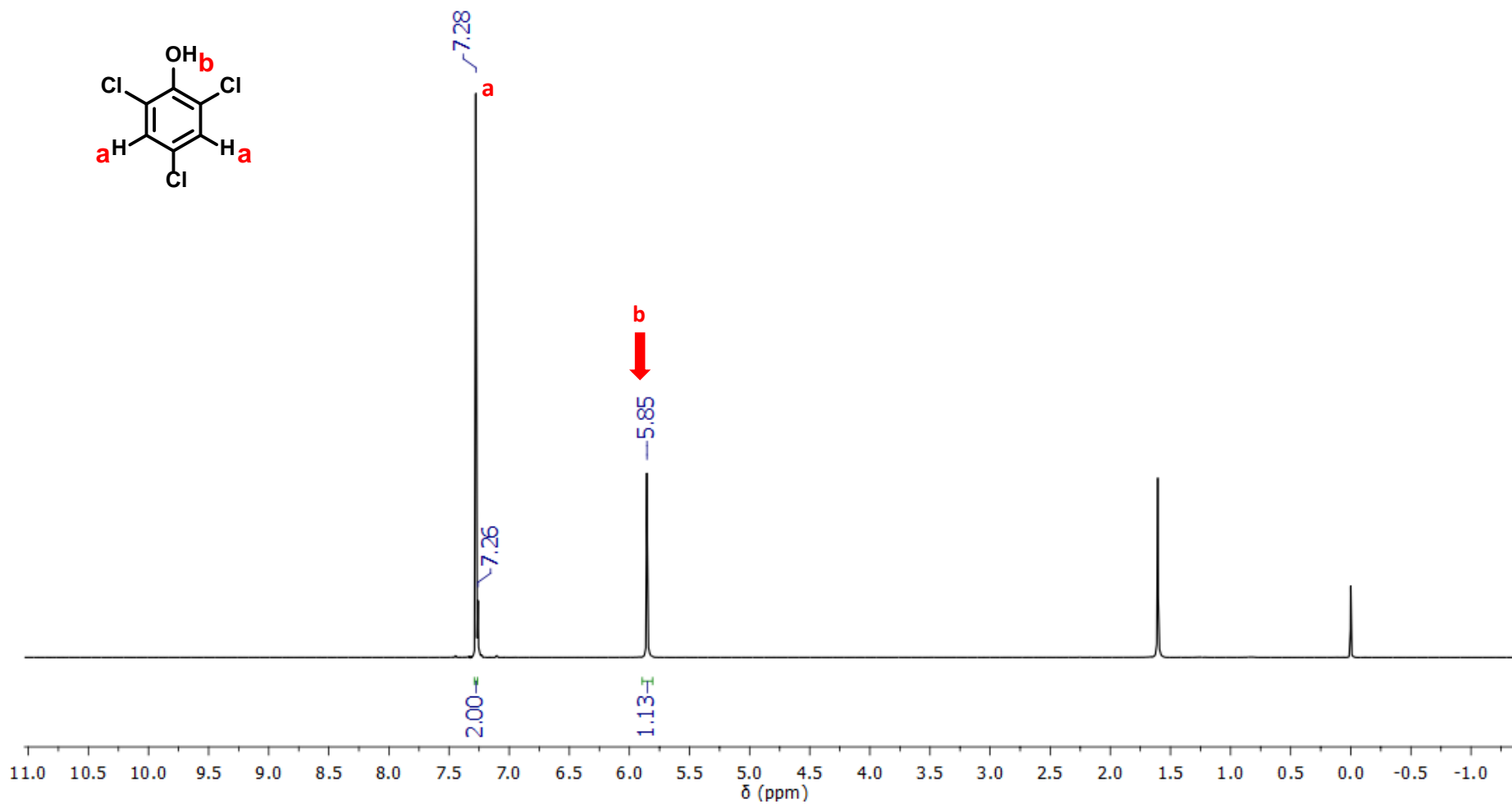


Fig. S16. ^1H NMR spectrum of 2,4,6-trichlorophenol in CDCl_3 .

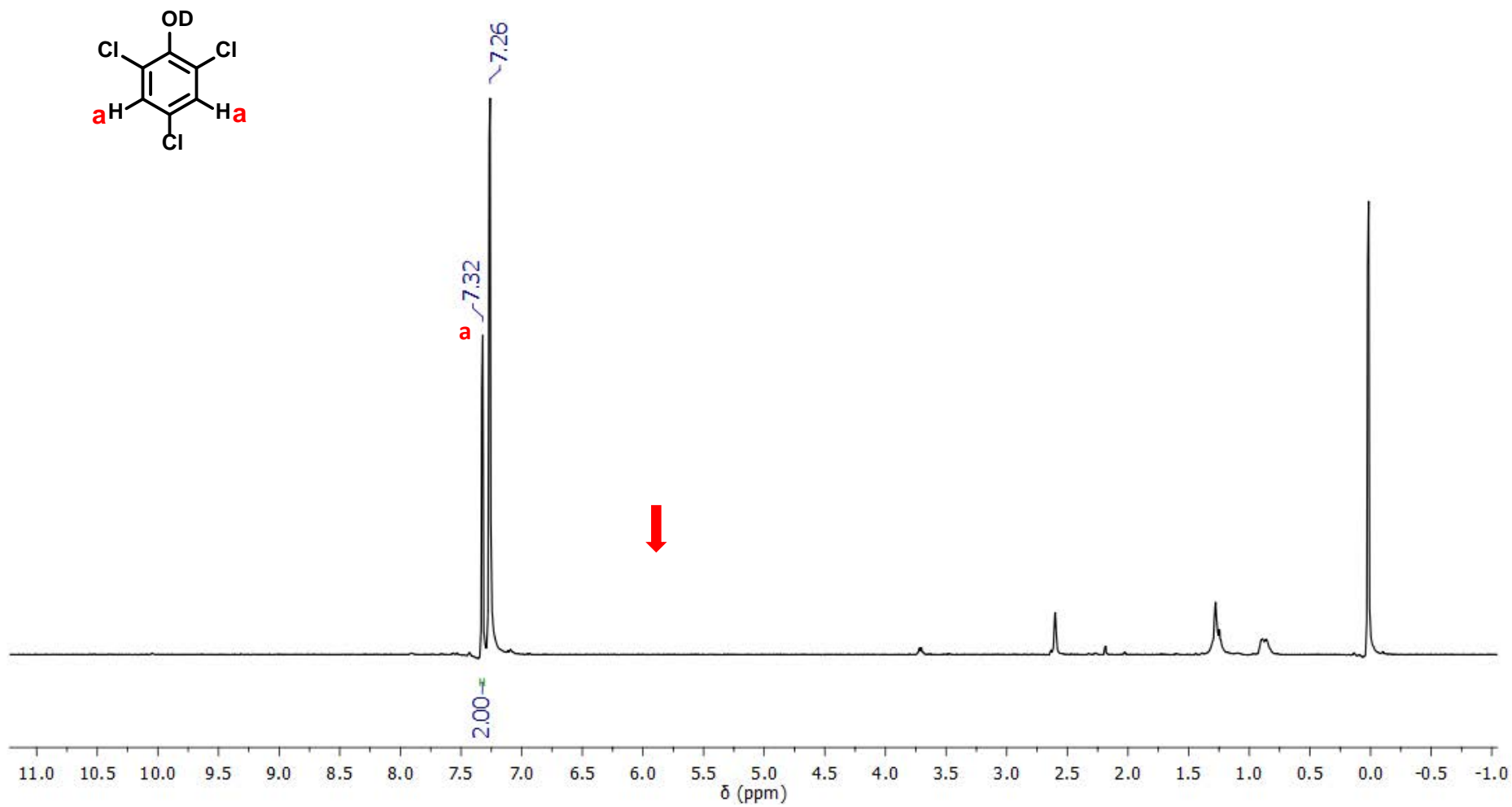


Fig. S17. ^1H NMR spectrum of 2,4,6-trichlorophenol-D in CDCl_3 .

References

1. Purification of Laboratory Chemicals, ed. W. L. F. Armarego and D. D. Perrin, Pergamon Press, Oxford, 1997.
2. C. R. Goldsmith, R. T. Jonas and T. D. P. Stack, *J. Am. Chem. Soc.*, 2002, **124**, 83.
3. W. K. C. Lo, C. J. McAdam, A. G. Blackman, J. D. Crowley and D. A. McMorrin, *Inorg. Chim. Acta*, 2015, **426**, 183.
4. A. A. Massie, M. C. Denler, L. T. Cardoso, A. N. Walker, M. K. Hossain, V. W. Day, E. Nordlander and T. A. Jackson, *Angew. Chem., Int. Ed.*, 2017, **56**, 4178.
5. A. A. Massie, A. Sinha, J. D. Parham, E. Nordlander and T. A. Jackson, *Inorg. Chem.*, 2018, **57**, 8253.
6. G. Mukherjee, C. W. Z. Lee, S. S. Nag, A. Alili, F. G. Cantú Reinhard, D. Kumar, C. V. Sastri and S. P. de Visser, *Dalton Trans.*, 2018, **47**, 14945.